Supporting Information

Clarke et al. 10.1073/pnas.1800165115

SI Materials and Methods

TRAP RNA Isolation. RNA was collected from hippocampi, striata, and cortex of *Aldh1l1-eGFP-L10a* mice based on published protocols (21, 22). Briefly, freshly dissected brain regions were collected from three animals for each age and individually homogenized. RNA was extracted from 20% of cleared lysate as input. The remaining lysate was incubated with freshly bound mouse anti-GFP antibody (19F7 and 19C8 clones; Memorial Sloan-Kettering Cancer Center Site) magnetic beads (Dynabeads Protein G beads; Thermo Fisher Scientific) with rocking for 2 h at 4 °C. The beads were washed three times in high-salt solution. RNA was purified from the IP and corresponding input samples using the RNeasy Plus kit (QIAGEN), according to the manufacturer's protocol. RNA concentration and quality were assessed with by Bioanalyzer analysis (Agilent Technologies). RNA samples with RNA integrity greater than 8 were used for library construction.

RNAseq Library Construction and Sequencing. RNAseq libraries were made from total RNA isolated from whole-brain input and TRAP-isolated samples. For first- and second-strand cDNA synthesis and single primer isothermal amplification, we used Ovation RNAseq system V2 (7102; Nugen) according to manufacturer's instructions, and fragmented cDNA with a Covaris S2 sonicator with duty cycle 10%, intensity 5, cycles/burst 100, for 5 min. We then used Next Ultra RNAseq library prep kit for Illumina (E7530; New England Biolabs) and NEBNext multiplex oligos for Illumina (E7335 and E7500; New England Biolabs) to perform end repair, adaptor ligation, and nine cycles of PCR enrichment according to manufacturer's instructions. Library quality was assessed by Bioanalyzer and qPCR, and high-quality libraries were sequenced by the Illumina NextSeq sequencer to obtain 75 bp paired-end reads.

RNAseq Analysis. We used https://usegalaxy.org to run the Tuxedo pipeline. We groomed the concatenated fastq files using FASTQ groomer (v 1.0.4), and aligned reads with Bowtie2 and identified splice junctions with TopHat, both using TopHat tool (v2.0.14, Galaxy v 0.9) with the following changes to default parameters: paired end data and mm9 mouse reference genome. For expression level estimation, we used TopHat accepted hits with Cufflinks (v 2.2.1, Galaxy v 2.2.1.0), with the following changes to default parameters: use reference genome mm9, "Yes" count hits compatible with reference RNAs only, and "Standard Length Correction" only. We downloaded gene expression (FPKM data) for each sample and merged these into Datasets S1–S4.

IPA. For pairwise comparisons between 10-wk- and 2-y-old astrocyte samples, we provided FPKM, log2(Fold Change), *P* values, and FDRs from Cufflink and edgeR analyses. We plotted significantly ($P < 0.05$) enriched pathways that were predicted to be either up- or down-regulated by IPA.

Microfluidics-Based qPCR. Total RNA was extracted from whole-brain or TRAP-isolated samples, cDNA synthesis was performed using the RNeasy Plus kit (Qiagen), and cDNA synthesis was performed using the SuperScript VILO cDNA synthesis kit (Invitrogen) according to supplier protocols. We designed primers using NCBI primer Basic Local Alignment Search Tool (BLAST) software (https://www.ncbi.nlm.nih.gov/tools/primer-blast/) and selected primer pairs with least probability of amplifying nonspecific products as predicted by NCBI primer BLAST. All primers had 90 to 105% efficiency. We designed primer pairs to amplify products that spanned exon–exon junctions to avoid amplification of genomic DNA. We tested the specificity of the primer pairs by PCR with mouse whole-brain cDNA (prepared fresh), and examined PCR products by agarose gel electrophoresis. For microfluidic qPCR, 1.25 μL of each cDNA sample was preamplified using 2.5 μL of 2× Taqman preamplification master mix (Applied Biosystems) and 1.25 μL of the primer pool (0.2 pmol each primer per microliter). Preamplification was performed using a 10-min 95 °C denaturation step and 14 cycles of 15 s at 95 °C and 4 min at 60 °C. Reaction products were diluted 5× in TE Buffer (Teknova). Five microliters from a sample mix containing preamplified cDNA and amplification Master mix (20 mM MgCl2, 10 mM dNTPs, FastStart Taq polymerase, DNA-binding dye loading reagent, 50× ROX, 20× Evagreen) was loaded into each sample inlet of a 96.96 Dynamic Array chip (Fluidigm Corporation), and 5 μL from an assay mix containing DNA-assay loading reagent, as well as forward and reverse primers (10 pmol·μL^{-1}) was loaded into each detector inlet. The chip was then placed in the NanoFlexTM 4-IFC Controller (Fluidigm) for loading and mixing. After loading, the chip was processed in the BioMark HD Real-Time PCR System (Fluidigm) using a cycling program of 10 min at 95 °C followed by 40 cycles of 95 °C for 15 s, 60 °C for 30 s, and 72 °C for 30 s. After completion of qPCR, a melting curve of amplified products was determined. Data were collected using BioMark Data Collection Software 2.1.1 build 20090519.0926 (Fluidigm) as the cycle of quantification, where the fluorescence signal of amplified DNA intersected with background noise. Fluidigm data were corrected for differences in input RNA using the mean of the reference gene Rplp0. Data preprocessing and analysis was completed using Fluidigm Melting Curve Analysis Software 1.1.0 build 20100514.1234 (Fluidigm) and Real-time PCR Analysis Software 2.1.1 build 20090521.1135 (Fluidigm) to determine valid PCR reactions. Invalid reactions were removed from later analysis. Quantitative RT-PCR was conducted following the minimum information for publication of quantitative real-time PCR experiments guidelines. The array accommodated reactions for 96 samples and 96 genes in total. The preamplified cDNA samples from the stimulation experiments were measured together with no reverse transcriptase and no template controls on 96.96 Dynamic Array chips (Fluidigm). Cell-type–specific transcripts were also detected for microglia, oligodendrocyte lineage cells, and neurons, with any astrocyte samples containing measurable levels of other cell types removed from further analysis. The primer sequences used were as follows: *C4B* (forward primer: GACAAGGCACCTTCAGAACC, reverse primer: CAGCAGCTTAGTCAGGGTTACA), *Stat3* (forward primer: GCCCCGTACCTGAAGACCAA, reverse primer: ACACTCCGAGGTCAGATCCA), and *C3* (forward primer: AGCTTCAGGGTCCCAGCTAC, reverse primer: GCTGGAATCTTGATGGAGACGC). All other primer sequences are detailed in ref. 9.

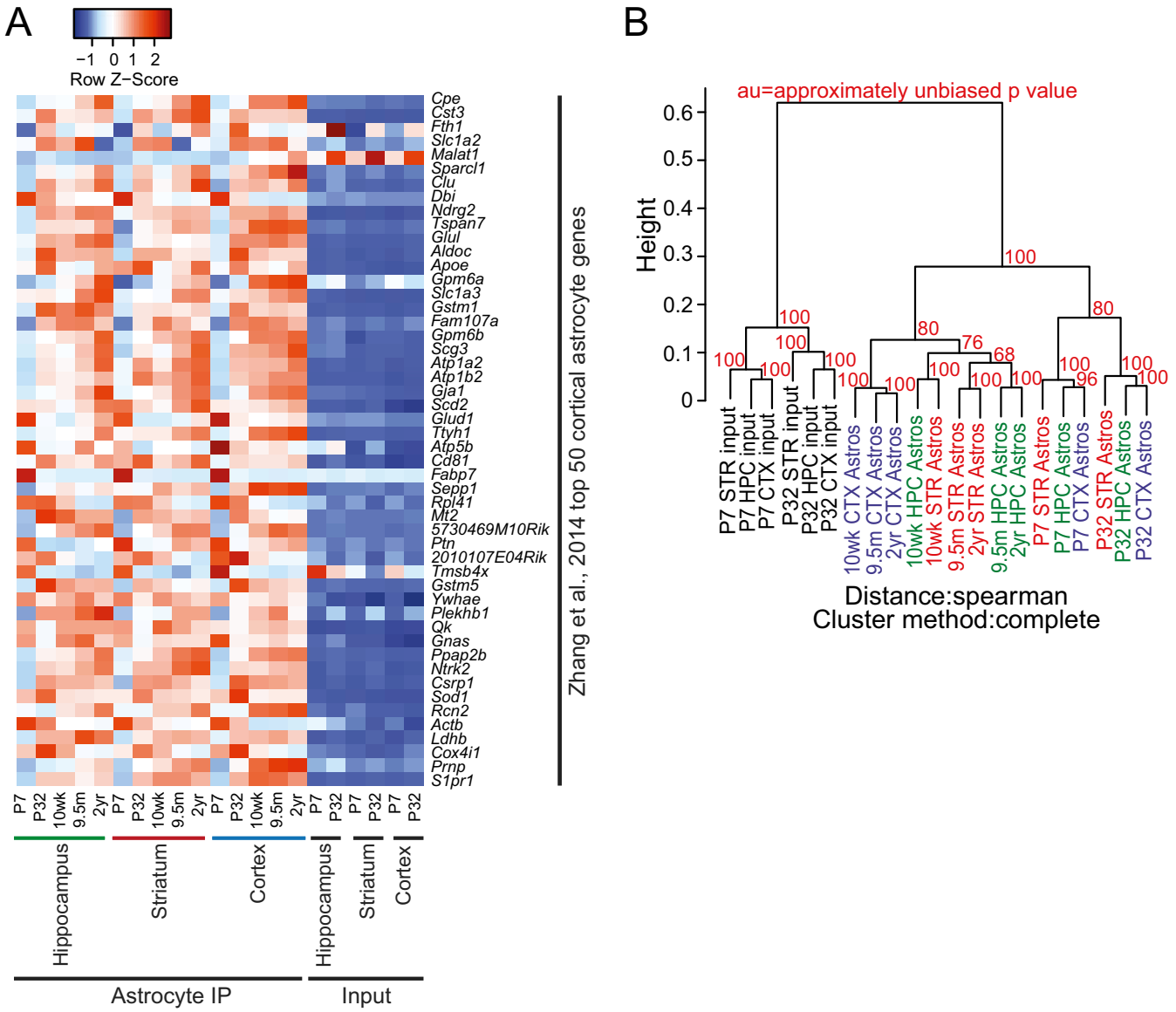

Fig. S1. Characterization of aging-induced transcriptional changes. (*A*) Heatmap representing mean FPKM for all RNAseq samples (replicates of three animals at P7, P32, 10 wk, and 2 y; replicates of two animals at 9.5 m) showing relative enrichment (red) or depletion (blue) of the 50 top cortical astrocyte genes from Zhang et al. (24). Row Z scores were calculated using FPKM. (*B*) Dendrogram of averaged expression data for genes with FPKM ≥ 5 in astrocyte and input samples from the hippocampus, striatum, and cortex. Spearman complete clustering was performed using the PVclust package (55). Red numbers depict approximately unbiased *P* value as calculated by PVclust. Astros, Astrocytes.

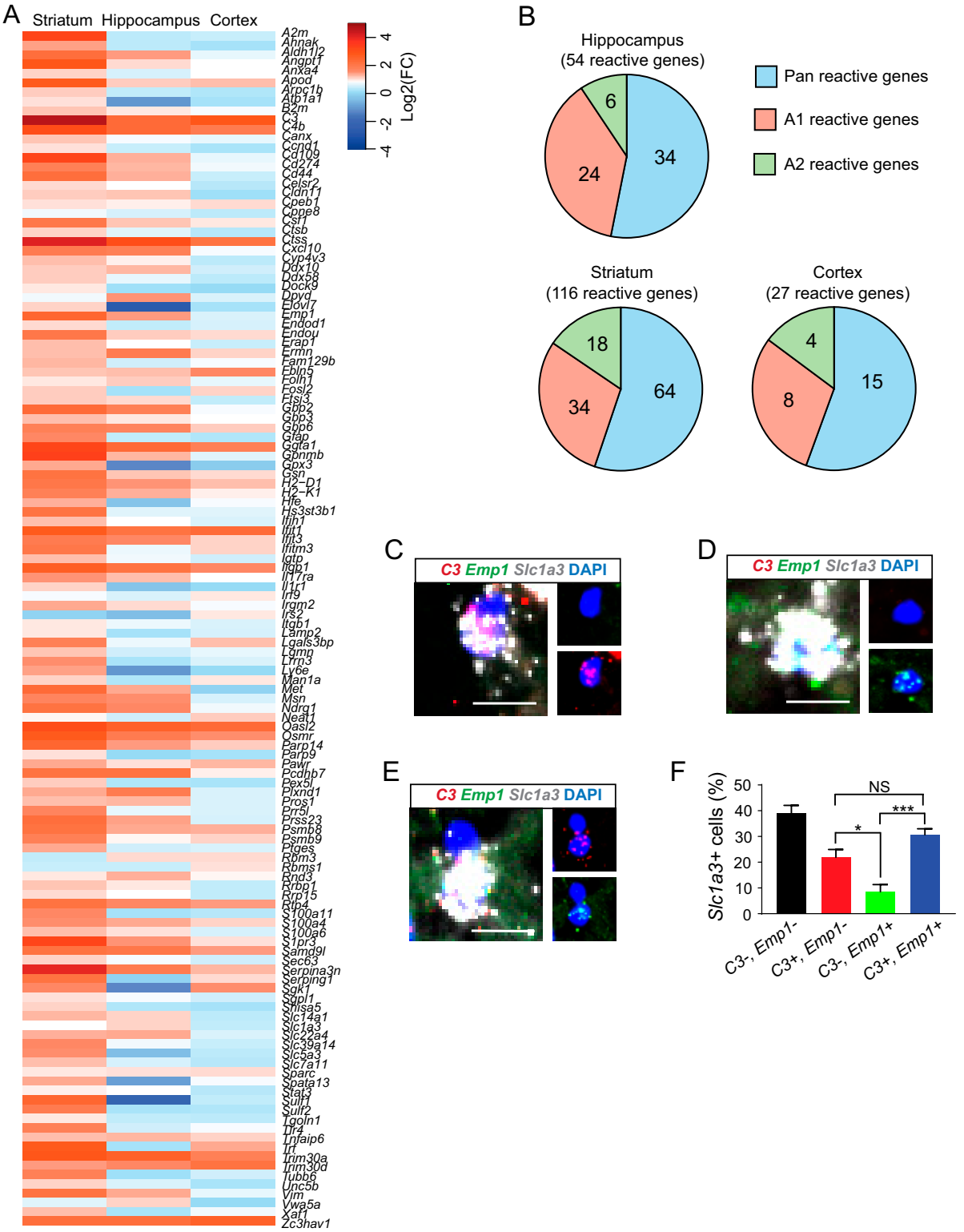

Fig. S2. Characterization of reactive gene changes. (*A*) Heatmap depicting the fold change of all significantly up-regulated ($P < 0.05$ in edgeR analysis) aging-induced reactive astrocyte genes in the hippocampus, striatum, and cortex. (*B*) Pie charts quantifying the total number of pan-reactive genes (genes induced by neuroinflammation and ischemia), A1 genes (genes specifically induced by neuroinflammation), and A2 genes (genes specifically induced by ischemia) significantly ($P < 0.05$) up-regulated in aged (2 y) astrocytes compared with adult (10 wk) astrocytes in the hippocampus, striatum, and cortex. (*C*) Representative in situ hybridization image of an *Slc1a3*+ astrocyte expressing the A1 reactive gene *C3*, in the 2-y-old striatum. (Scale bar, 10 μm.) (*D*) Representative in situ hybridization image of an *Slc1a3*+ astrocyte expressing the A2 reactive gene *Emp1*, in the 2-y-old striatum. (Scale bar, 10 μm.) (*E*) Representative in situ hybridization image of an *Slc1a3*+ astrocyte expressing both the A1 reactive gene *C3* and the A2 reactive gene *Emp1*, in the 2-y-old striatum. (Scale bar, 10 μm.) (*F*) Bar chart depicting quantification of the number of *Slc1a3*+ astrocytes expressing no detectable levels of reactive genes, detectable levels of A1 reactive astrocyte gene *C3*, detectable levels of A2 reactive astrocyte gene *Emp1*, and detectable levels of both A1 (*C3*) and A2 (*Emp1*) genes in aged (2 y old) striatum. Error bars depict mean ± SEM. ***$P < 0.001$; *$P < 0.05$; $n = 3$ animals.

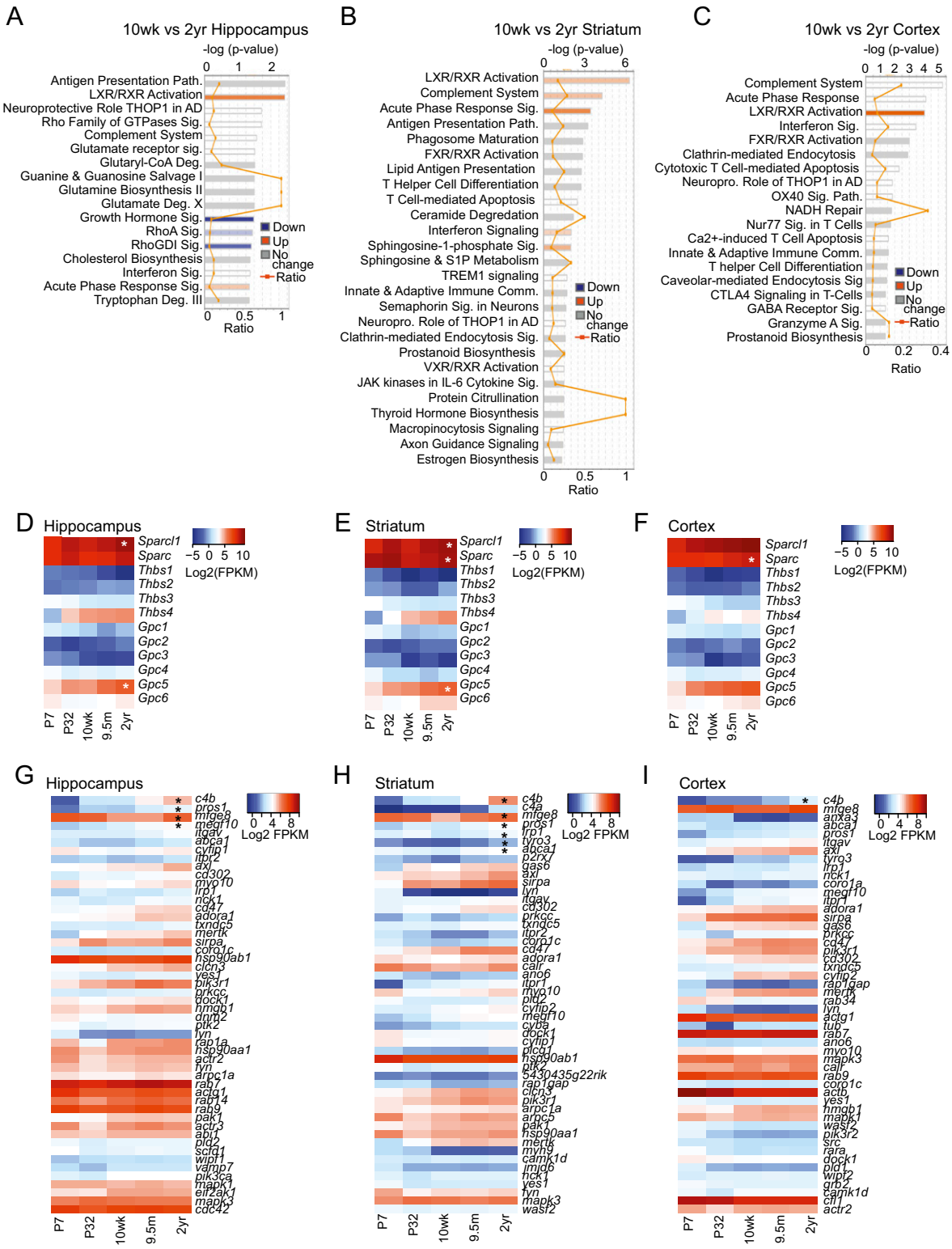

Fig. S3. Analysis of IPA pathways, synaptogenic and phagocytic pathways in aged astrocytes. (*A–C*) Enriched pathways in adult (10 wk) to aged (2 y) astrocytes with $P < 0.01$ and absolute Z score ≥ 1 in the (*A*) hippocampus, (*B*) striatum, and (*C*) cortex, adapted from QIAGEN's IPA technology. Ratio refers to genes detected/genes per pathway. (*D–F*) Heatmaps comparing the mean expression of synaptogenic transcripts in TRAP astrocyte RNA samples isolated from the (*D*) hippocampus, (*E*) striatum, and (*F*) cortex of P7, P32, 10-wk-, 9.5-mo-, and 2-y-old mice. Asterisks (*) denote significantly ($P < 0.05$) increased expression in 2 y old samples compared with 10 wk by edgeR analysis. (*G–I*) Heatmaps comparing the mean expression of phagocytic transcripts in TRAP astrocyte RNA samples isolated from the (*G*) hippocampus, (*H*) striatum, and (*I*) cortex of P7, P32, 10-wk-, 9.5-mo-, and 2-y-old mice. Asterisks (*) denote significantly ($P < 0.05$) increased expression in 2-y-old samples compared with 10 wk by edgeR analysis.

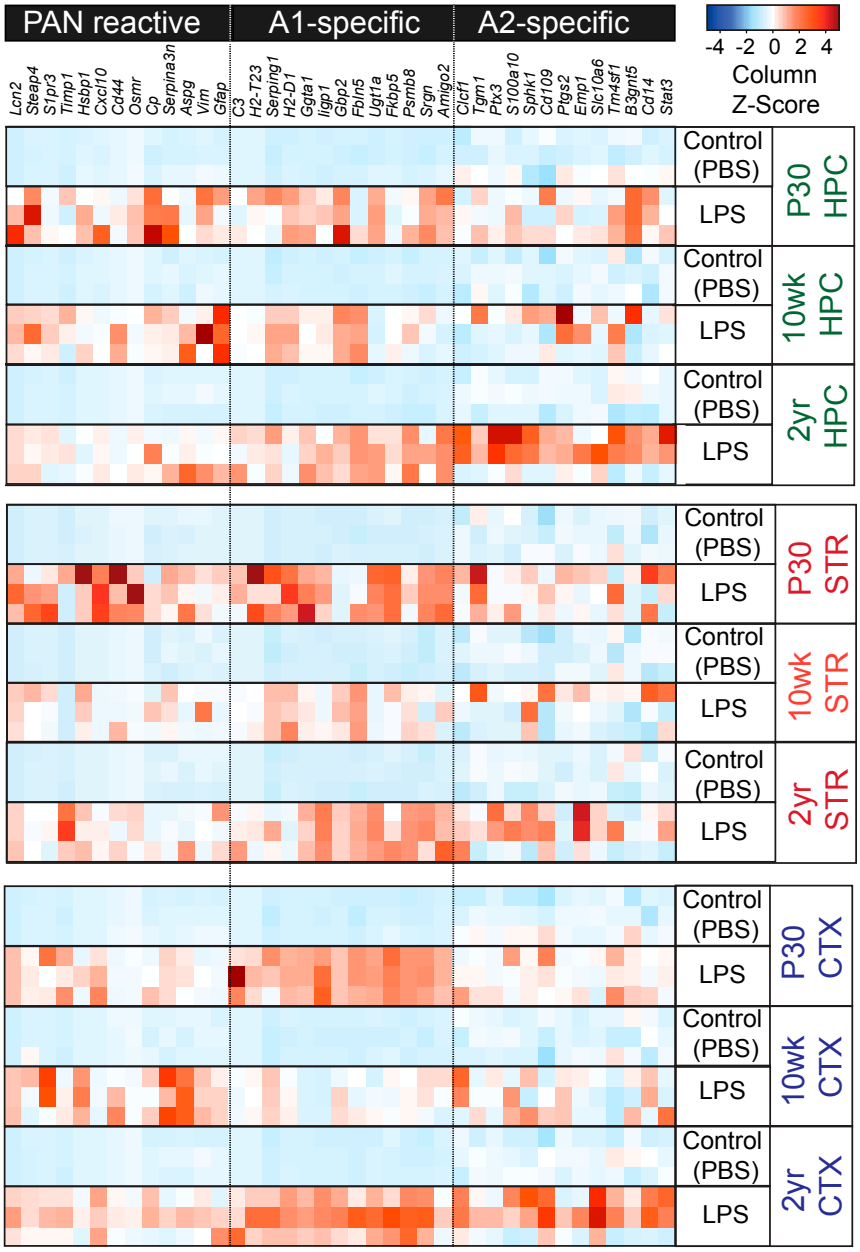

Fig. S4. Heatmaps of the fold change in astrocyte LPS response with age by microfluidics-based qPCR. Heatmap depicting fold change in pan-reactive (genes induced by neuroinflammation or ischemia), A1-reactive (genes induced by neuroinflammation), and A2-reactive (genes induced by ischemia) genes in TRAP-isolated astrocyte samples 24 h after 5 mg/kg LPS treatment compared with PBS-injected mice at P30, 10 wk, and 2 y of age, in the hippocampus (HPC), striatum (STR), and cortex (CTX).

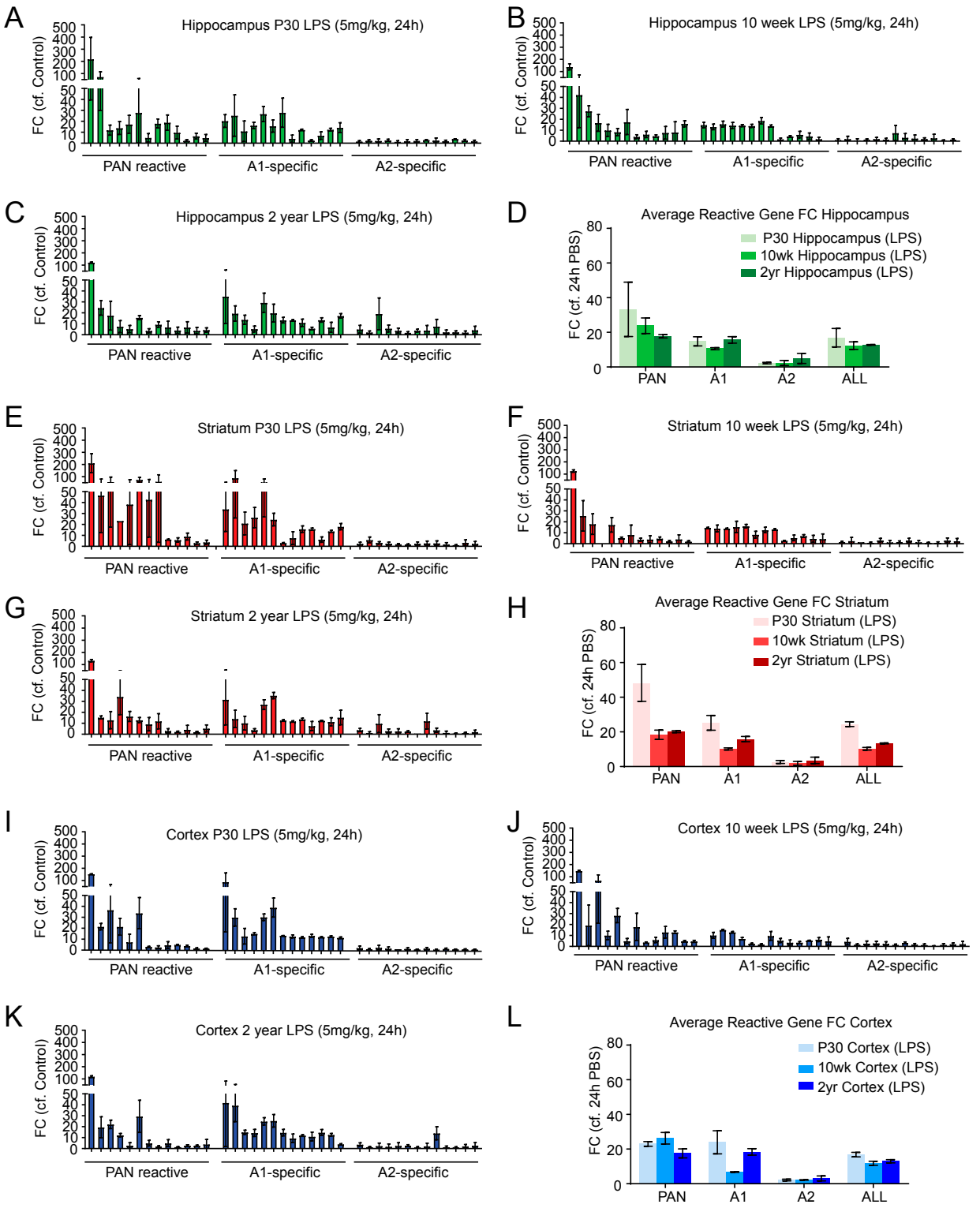

Fig. S5. Comparison of the astrocyte LPS response with age by microfluidics-based qPCR. (*A–C*) Quantification of the fold induction of pan-reactive, A1-specific, and A2-specfic transcripts in response to LPS injection (5 mg/kg), compared with PBS-injected control mice, in hippocampal astrocyte RNA samples isolated by TRAP at (*A*) P30, (*B*) 10 wk, and (*C*) 2 y. (*D*) Bar plot quantifying the average fold induction of all pan-reactive, A1-specific, A2-specific, and reactive transcripts 24 h after LPS injection (5 mg/kg) in hippocampal astrocyte RNA samples isolated by TRAP at three ages (P30, 10 wk, and 2 y). (*E–G*) Quantification of the fold induction of pan-reactive, A1-specific, and A2-specfic transcripts in response to LPS injection (5 mg/kg), compared with PBS-injected control mice, in striatal astrocyte RNA samples isolated by TRAP at (*E*) P30, (*F*) 10 wk, and (*G*) 2 y. (*H*) Bar plot quantifying the average fold induction of all pan-reactive, A1-specific, A2-specific, and reactive transcripts 24 h after LPS injection (5 mg/kg) in striatal astrocyte RNA samples isolated by TRAP at three ages (P30, 10 wk, and 2 y). (*I–K*) Quantification of the fold induction of pan-reactive, A1-specific, and A2-specfic transcripts in response to LPS injection (5 mg/kg), compared with PBS-injected control mice, in cortical astrocyte RNA samples isolated by TRAP at (*I*) P30, (*J*) 10 wk, and (*K*) 2 y. (*L*) Bar plot quantifying the average fold induction of all pan-reactive, A1-specific, A2-specific, and reactive transcripts 24 h after LPS injection (5 mg/kg) in cortical astrocyte RNA samples isolated by TRAP at three ages (P30, 10 wk, and 2 y). Error bars depict mean ± SEM.

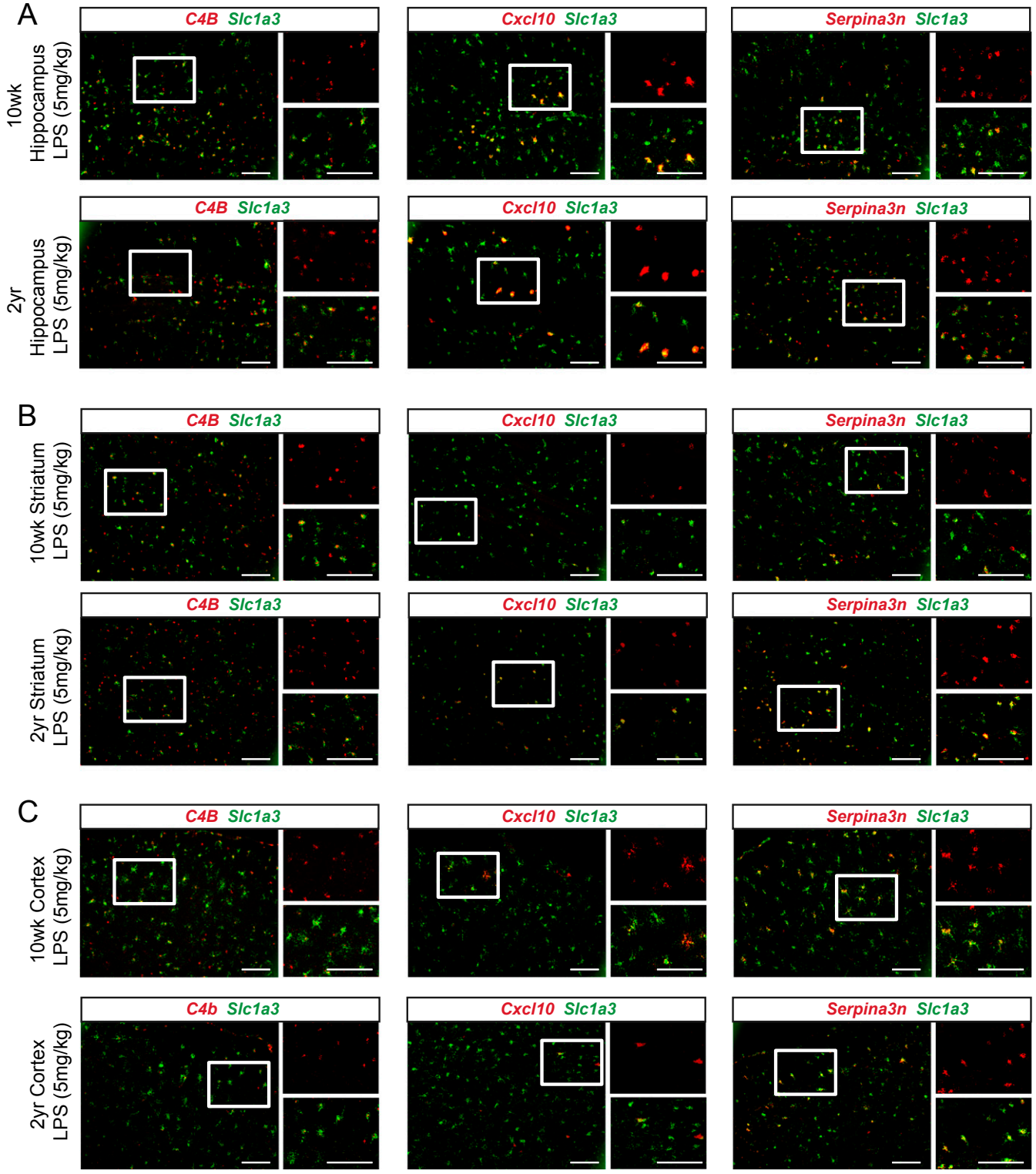

Fig. S6. Comparison of astrocyte LPS response with age by in situ hybridization. Shown are representative in situ hybridization images for three aging-induced astrocyte genes (*Serpina3n*, *C4B*, and *Cxcl10*) showing colocalization with the astrocyte marker *Slc1a3* in adult (10 wk) and aged mice (2 y) in the (*A*) hippocampus, (*B*) striatum, and (*C*) cortex 24 h after LPS (5 mg/kg) injection. (Scale bar, 100 μm.)

Dataset S1. Differentially expressed genes in aged hippocampal astrocytes

Dataset S1

Differentially expressed genes (FDR < 0.05) between 10-wk- and 2-y-old hippocampal astrocytes (genes were filtered for FPKM ≥ 5 in 2-y-old samples for up-regulated genes, and FPKM ≥ 5 in 10-wk-old samples for down-regulated genes); FDR, False discovery rate; log2(FC), log2(Fold Change between 10-wk- and 2-y-old astrocytes); logCPM, log counts per million

Dataset S2. Differentially expressed genes in aged striatal astrocytes

Dataset S2

Differentially expressed genes (FDR < 0.05) between 10-wk- and 2-y-old striatal astrocytes (genes were filtered for FPKM ≥ 5 in 2-y-old samples for up-regulated genes, and FPKM ≥ 5 in 10-wk-old samples for down-regulated genes).

Dataset S3. Differentially expressed genes in aged cortical astrocytes

Dataset S3

Differentially expressed genes (FDR < 0.05) between 10-wk- and 2-y-old cortical astrocytes (genes were filtered for FPKM ≥ 5 in 2-y-old samples for up-regulated genes, and FPKM ≥ 5 in 10-wk-old samples for down-regulated genes).

Dataset S4. RNAseq data for all astrocyte samples across the mouse lifespan

Dataset S4

FPKM values are listed for each gene (GeneID column) for each replicate of all brain regions and ages. Each column represents one replicate for either an astrocyte sample or input sample. Data for each brain region are separated into three separate tabs and labeled as hippocampus, striatum, and cortex; Astro, astrocyte; rep, replicate